

Nano-Encapsulation of Plitidepsin: *In Vivo* Pharmacokinetics, Biodistribution, and Efficacy in a Renal Xenograft Tumor Model

Hugo Oliveira · Julie Thevenot · Elisabeth Garanger · Emmanuel Ibarboure · Pilar Calvo · Pablo Aviles · Maria Jose Guillen · Sébastien Lecommandoux

Received: 27 June 2013 / Accepted: 22 September 2013 / Published online: 28 November 2013
© Springer Science+Business Media New York 2013

ABSTRACT

Purpose Plitidepsin is an antineoplastic currently in clinical evaluation in a phase III trial in multiple myeloma (ADMYRE). Presently, the hydrophobic drug plitidepsin is formulated using Cremophor®, an adjuvant associated with unwanted hypersensitivity reactions. In search of alternatives, we developed and tested two nanoparticle-based formulations of plitidepsin, aiming to modify/improve drug biodistribution and efficacy.

Methods Using nanoprecipitation, plitidepsin was loaded in polymer nanoparticles made of amphiphilic block copolymers (i.e. PEG-*b*-PBLG or PTMC-*b*-PGA). The pharmacokinetics, biodistribution and therapeutic efficacy was assessed using a xenograft renal cancer mouse model (MRI-H-121 xenograft) upon administration of the different plitidepsin formulations at maximum tolerated multiple doses (0.20 and 0.25 mg/kg for Cremophor® and copolymer formulations, respectively).

Results High plitidepsin loading efficiencies were obtained for both copolymer formulations. Considering pharmacokinetics, PEG-*b*-PBLG formulation showed lower plasma clearance, associated with higher AUC and C_{max} than Cremophor® or PTMC-*b*-PGA formulations. Additionally, the PEG-*b*-PBLG formulation presented lower liver and kidney accumulation compared with the other two formulations, associated with an equivalent tumor distribution. Regarding the anticancer activity, all formulations elicited similar efficacy profiles, as compared to the Cremophor® formulation, successfully reducing tumor growth rate.

Conclusions Although the nanoparticle formulations present equivalent anticancer activity, compared to the Cremophor® formulation, they show improved biodistribution profiles, presenting novel tools for future plitidepsin-based therapies.

KEY WORDS cancer therapy · drug delivery · nanomedicine · plitidepsin · polymersomes

Electronic supplementary material The online version of this article (doi:10.1007/s11095-013-1220-3) contains supplementary material, which is available to authorized users.

P. Calvo · P. Aviles · M. J. Guillen
Pharma Mar S.A., Sociedad Unipersonal, Colmenar Viejo, Madrid, Spain

H. Oliveira · J. Thevenot · E. Garanger · E. Ibarboure ·
S. Lecommandoux
Université de Bordeaux/IPB, ENSCBP, 16 avenue Pey Berland
33607 Pessac Cedex, France

H. Oliveira (✉) · J. Thevenot · E. Garanger · E. Ibarboure ·
S. Lecommandoux (✉)
CNRS, Laboratoire de Chimie des Polymères Organiques
(UMR5629), 16 Avenue Pey Berland, 33607 Pessac Cedex, France
e-mail: hugo.de-oliveira@inserm.fr
e-mail: lecommandoux@enscbp.fr

Present Address:

H. Oliveira
BIOTIS, Inserm U1026, Zone Nord, Bât. 4a, 2ème étage, 146 rue Léo
Saignat, 33076 Bordeaux Cedex, France

ABBREVIATIONS

CEW	Cremophor®:Ethanol:Water (15:15:70 v/v/v)
CLp	Clearance
C _{max}	Maximum concentration
CRE	Cremophor®
FWR	Feed Weight Ratio
HPLC	High performance liquid chromatography
iv.	Intravenous
LC	Loading content
LE	Loading efficiency
MTD	Maximum tolerated dose
PEG- <i>b</i> -PBLG	Poly(ethylene glycol)-block-poly (γ-benzyl-L-glutamate)
PTMC- <i>b</i> -PGA	Poly(trimethylene carbonate)-block-poly (glutamic acid)
SD	Standard deviation
t _{1/2}	Terminal half-life time
V _{dss}	Apparent volume of distribution at steady state

INTRODUCTION

During the last decades a huge effort has been devoted to the development of novel and more efficient cancer therapeutic tools. In that sense, nanotechnology has been leading the way, with a wide range of systems in pre-clinical testing or already applied for treatment (1,2). Indeed, the American National Cancer Institute has associated nanotechnology to a potential paradigm shift on cancer prevention, detection and treatment. Biodegradable polymeric particles made from hydrophilic-hydrophobic diblock copolymers are especially attractive for drug delivery as they can achieve controlled, sustained and targeted delivery (3). The hydrophobic block forms the nanoparticle inner core, creating a reservoir for hydrophobic drugs, and the hydrophilic block can render the nanoparticle stealth or increase its stability in the body.

Plitidepsin (Aplidin®) is a cyclic depsipeptide originally isolated from the mediterranean tunicate *Aplidium albicans* and currently produced by chemical synthesis (4). Plitidepsin has been developed as an antineoplastic compound based on the activities shown in preclinical studies using both cell lines and murine models of a wide variety of different tumors (5–7). The mechanism of action of plitidepsin suggests an induction of oxidative stress, increasing oxidation levels of cell membrane phospholipids and DNA (8), decreasing intracellular levels of glutathione and activating the Rac1-JNK pathway, resulting in caspase-dependent and -independent cell apoptosis (9,10). Plitidepsin has been extensively applied as single-agent chemotherapy in phase I and II clinical trials (11–21), with significant antitumor activity observed for a wide number of solid tumors as well as haematological malignancies. Plitidepsin is currently under clinical evaluation in a phase III trial for multiple myeloma (ADMYRE). Due to its inherent hydrophobicity (i.e. LogP: >5) plitidepsin is nearly insoluble in aqueous media and needs to be associated with an adjuvant in order to permit *iv.* administration. In that sense, plitidepsin is presently formulated using Cremophor® (CRE), an adjuvant that permits an important increase of solubility but nevertheless associated with unwanted biological effects. Although the use of surfactants like Tween 80 and CRE significantly increase drug solubility and permit intravenous administration, these agents have shown to be responsible for acute hypersensitivity reactions (22,23). Such an example is the CRE-formulated single-agent paclitaxel (Taxol®; Bristol-Myers Squibb Co., Princeton, New Jersey), where CRE is responsible for hypersensitivity reactions and where premedication with steroid and antihistaminic drugs is required in order to minimize this side effect (24).

In search of alternatives, we developed and tested nanoparticle-based formulations of plitidepsin, aiming to modify/improve biodistribution and efficacy in a renal cancer treatment scenario. Hence, here we propose two polymer-based nanoparticle systems, vesicular and micellar, as alternative approaches for plitidepsin delivery *in vivo*. Poly(ethylene glycol)-*block*-

poly(γ -benzyl-L-glutamate) (PEG-*b*-PBLG) copolymer forms micellar structures, whereas poly(trimethylene carbonate)-*block*-poly(glutamic acid) (PTMC-*b*-PGA) form vesicular structures, for the chosen block lengths. These copolymers allow the solubilization of hydrophobic drugs, like plitidepsin, and may provide their sustained release while improving their biodistribution profile. Additionally, the stealth character of the PEG moieties may prevent the interactions with cells and proteins, increasing drug circulation time (25).

MATERIALS AND METHODS

Materials

Plitidepsin was produced by proprietary chemical synthesis by Pharmamar and formulated using a Cremophor:Ethanol:Water (15:15:70 %; v/v/v) mixture (CEW), as previously described (26), or encapsulated in nanoparticle systems as described hereafter.

Solvents, dimethyl sulfoxide (DMSO), dimethyl formamide (DMF), diethyl ether, were of synthesis grade and used as received unless otherwise mentioned. Water was of ultrapure grade (type 1). Tris(hydroxymethyl)aminomethane (Trizma®) and sodium chloride were purchased from Sigma and used as received. Amphiphilic block copolymers, PEG-*b*-PBLG and PTMC-*b*-PGA, were synthesized according to previously published methods, as follows. PEG-*b*-PBLG (2.0-*b*-2.8) was synthesized following the protocol described by Barbosa *et al.* with minor modifications (27). Briefly, CH₃O-PEG-NH₂ (2,000 g/mol, RAPP Polymere, Germany; 2 g, 1 mM) was dissolved in 2 ml dioxane, freeze-dried and dissolved in dry DMF (0.1 g/ml). In a glovebox, γ -benzyl-L-glutamate N-carboxyanhydride (Isochem, France; 4.20 g, 16 mM) was introduced into a flame-dried Schlenk flask and dissolved in anhydrous DMF (0.1 g/ml). This solution was then added under vacuum to the first flask. The mixture was stirred for 48 h at 40°C in an oil bath. The polymerization medium was concentrated by cryo-distillation and the copolymer was recovered by precipitation into cold diethyl ether. The white powdery solid was then washed three times with diethyl ether and finally dried under dynamic vacuum for 24 h. The degree of polymerization of PBLG measured by proton NMR was DP = 13 ± 1, corresponding to a molar mass of 2.8 ± 0.2 kg/mol.

PTMC-*b*-PGA (2.5-*b*-1.5) diblock copolymer was synthesized following a method previously published by our group (28). Briefly, amino end-functionalised PTMC (PTMC-NH₂) was first synthesized by ring-opening polymerization (ROP) of TMC (kindly provided by Labso Chimie Fine, Blanquefort, France) in the presence of diethyl zinc and 3-(Fmoc-amino)-1-propanol as initiator, followed by the deprotection of the amine group with piperidin. PTMC-*b*-PBLG was then prepared by ROP of γ -benzyl-L-glutamate N-carboxyanhydride initiated by the PTMC-NH₂ macroinitiator and subsequently

deprotected into PTMC-*b*-PGA amphiphilic diblock copolymer by catalytic hydrogenation. The final degrees of polymerization and corresponding molar masses of each block were calculated from proton NMR: PTMC block, DP = 25 ± 1 (Mn = 2.5 kg/mol), PGA block, DP = 12 ± 1 (Mn = 1.5 kg/mol).

Definitions

Drug feed weight ratio, loading efficiency and loading content are defined as follows:

$$\text{Feed Weight Ratio (FWR)} = \frac{\text{mass of drug engaged}}{\text{mass of polymer}} \cdot 100$$

$$\text{Loading Efficiency (LE)} = \frac{\text{mass of loaded drug}}{\text{mass of drug engaged}} \cdot 100$$

$$\text{Loading Content (LC)} = \frac{\text{mass of loaded drug}}{\text{mass of polymer}} \cdot 100$$

Drug-Loaded PEG-*b*-PBLG Nanoparticles Preparation

Suspensions of PEG-*b*-PBLG nanoparticles loaded with plitidepsin were prepared by the solvent-assisted self-assembly process, under sterile conditions. In a 500 ml round bottom flask, ultrapure water (120 ml) was added in 25 s to a solution of PEG-*b*-PBLG in DMSO (40 ml at 1.5 mg/ml) containing plitidepsin at different feed weight ratios (0–30% w/w). The addition was performed under magnetic stirring (250 rpm) at room temperature (22–25°C). Nanoparticle suspensions were purified by dialysis against ultrapure water and concentrated by ultrafiltration (MWCO 100,000 g/mol, Millipore).

Drug-Loaded PTMC-*b*-PGA Nanoparticles Preparation

Plitidepsin-loaded PTMC-*b*-PGA vesicles were prepared, under sterile conditions, by quickly adding (10 s) 60 mL Tris buffer 50 mM at pH 7.4 to 10 mL of PTMC-*b*-PGA (10 mg/mL) containing plitidepsin at different feed weight ratios (0–50% w/w) in DMSO under magnetic stirring (500 rpm). Excess drug and DMSO were removed by dialysis (3×: 4 h; RT; MWCO 3,500 g/mol) against saline Tris buffer (10 mM Tris, pH 7.4, ionic strength 150 mM). The process being very reproducible, it was repeated in different batches and the dispersion was concentrated by ultrafiltration (MWCO 100,000 g/mol MWCO 100,000 g/mol, Millipore).

Particle Characterization

Particles were characterized by dynamic light scattering (DLS) for hydrodynamic size measurement (Nano ZS90, Malvern

Instruments), and by transmission electron microscopy (TEM) and atomic force microscopy (AFM) for morphology assessment.

The exact polymer concentrations of the final dispersions were determined by measuring the solid content by differential weighing of an exact volume of suspension before and after drying using thermogravimetric analysis (TGA) as a microbalance.

Plitidepsin loading content (LC) and loading efficiency (LE) were determined by means of HPLC, against a plitidepsin calibration curve. For this purpose, an aliquot of nanoparticle dispersion (e.g. 2 ml at 1 mg/ml) was freeze-dried and the drug extracted using methanol. Samples were analyzed by HPLC using the following method: gradient 52% Acetonitrile 0.04% TFA for 23 min, 100% Acetonitrile 0.04% TFA for 15 min (40 min run time), flow 1 ml/min, injection volume 20 µl, detection wavelength λ = 270 nm.

Animal Experiments

Animals

Female athymic nu/nu and CD1 mice between 4 to 6 weeks of age (18–30 g) were purchased from Harlan Laboratories Models, S.L. (Barcelona, Spain). Animals were housed in individually ventilated cages (Sealsafe® Plus, Techniplast S.P.A.), 10 mice per cage, on a 12-h light–dark cycle at 21–23°C and 40–60% humidity. Mice were allowed free access to irradiated standard rodent diet (Tecklad 2914C) and sterilized water. Animal protocols were reviewed and approved according to regional Institutional Animal Care and Use Committees.

Tumor Implantation

Athymic nu/nu female mice were subcutaneously implanted at 4–6 weeks of age with Matrigel™-embedded fragments (3 mm³) of a human renal carcinoma, MRI-H-121 (DTP, DCTD Tumor Repository, Maryland, USA). When tumors reached ca. 200–300 mm³, tumor-bearing animals were randomly allocated into experimental groups.

Maximum Tolerated Dose Determination

The acute toxicity of the nanoparticle based formulations was determined by assessing the maximum tolerated multiple dose (MTMD)—corresponding to the highest dose, after 2 cycles of 5 consecutive treatment days, not to cause unacceptable side effects and body weight loss exceeding 20% in healthy CD1 female mice. Plitidepsin loaded copolymer nanoparticles were tested from 1.5 to 0.0 mg/kg, for PTMC-*b*-PGA and PEG-*b*-PBLG. Plitidepsin in the reference formulation (i.e.

Table 1 Characterization of Developed Plitidepsin-Loaded Nanoparticles Based on poly(ethylene glycol)-*block*-poly(γ -benzyl-L-glutamate) (PEG-*b*-PBLG) and poly(trimethylene carbonate)-*block*-poly(glutamic acid) (PTMC-*b*-PGA) Copolymers (Average \pm SD, $n=3$). Dh: Mean Hydrodynamic Diameter Obtained by DLS. PDI: Polydispersity Index. FWR, LC and LE are Defined in the "Materials and Methods"

Plitidepsin FWR (% w/w)	LC (% w/w)	LE (%)	Dh (nm)	PDI
PEG-<i>b</i>-PBLG				
0	–	–	157 \pm 19	0.19 \pm 0.02
10	7 \pm 1	66 \pm 6	129 \pm 14	0.14 \pm 0.02
30	22 \pm 2	74 \pm 8	164 \pm 23	0.21 \pm 0.04
PTMC-<i>b</i>-PGA				
0	–	–	111 \pm 6	0.05 \pm 0.01
10	8 \pm 1	77 \pm 12	119 \pm 5	0.04 \pm 0.01
20	15 \pm 1	77 \pm 7	165 \pm 11	0.16 \pm 0.04
40	34 \pm 1	86 \pm 3	165 \pm 11	0.13 \pm 0.04
50	41 \pm 1	81 \pm 1	167 \pm 6	0.13 \pm 0.01

Cremophor® EL/ethanol/water 15/15/70 w/w/w; CEW) was studied as a benchmark, and tested at 1.5 to 0.0 mg/kg using the same administration regime. Empty nanoparticles (PTMC-*b*-PGA and PEG-*b*-PBLG) were tested using the

same administration regime. Groups of 5 animals were used per each dose level.

Pharmacokinetics

Pharmacokinetic evaluation of plitidepsin was performed in MRI-H-121 cell tumor bearing athymic nu/nu female mice after a single intravenous bolus administration of CEW based plitidepsin (drug dose: 0.20 mg/Kg) or PEG-*b*-PBLG or PTMC-*b*-PGA based formulations (drug dose: 0.25 mg/Kg). Four animals were used per time point and formulation ($n=72$). At 30 min, 1, 2, 4, 8 and 24 h post-dosing the corresponding blood samples were collected from euthanized mice, in suitable polypropylene blood collection tubes containing EDTA. Blood samples were centrifuged at 3,000 rpm for 15 min at ca. 4°C and the resulting plasma was frozen at –20°C until further use. At the same time points tumor, kidney, liver, breast, intestine and spleen samples were harvested, weighed and frozen at –20°C until bioanalysis. Bioanalysis consisted of a supported-liquid extraction (SLE) followed by a gradient reversed phase chromatography and detection by positive ion electrospray tandem mass spectrometry (ESI/MS/MS) using multiple reaction monitoring (MRM).

Fig. 1 PTMC-*b*-PGA vesicles at 20% FWR plitidepsin (**a**) and PEG-*b*-PBLG particles at 30 wt.% FWR plitidepsin (**b**) observed by TEM after negative staining (uranyl acetate 1% w/v). Bar: 200 nm. DLS analysis showing correlation curves and size distribution (obtained from cumulant analysis) for PTMC-*b*-PGA vesicles at 20% FWR plitidepsin (**c**) and PEG-*b*-PBLG particles at 30 wt.% FWR plitidepsin (**d**).

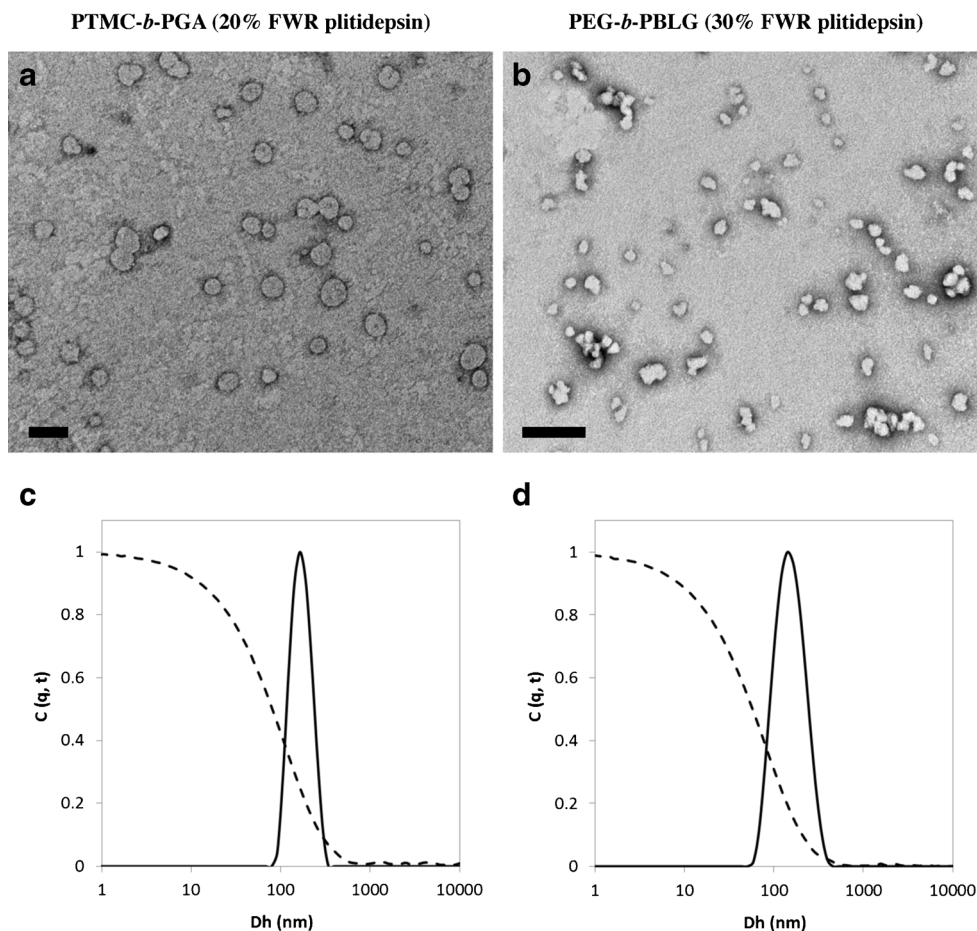


Table II Maximum Tolerated Repeated Dose (MTMD) for Plitidepsin-Loaded Particles and Cremophor® (CEW) Plitidepsin Formulation after 2 cycles of 5 Consecutive Days Administration in Female CD1 Mice (Expressed as mg of Plitidepsin per kg of Animal). Plitidepsin Loading Contents were 15 and 22 wt.% for PTMC-*b*-PGA Vesicles and PEG-*b*-PBLG Particles Respectively

	MTMD (mg/kg)
CEW	0.20
PTMC- <i>b</i> -PGA	0.30
PEG- <i>b</i> -PBLG	0.25

Antitumor Activity

In vivo antitumor activity was evaluated in MRI-H-121 cell tumor bearing athymic nu/nu female mice following five consecutive daily doses (day 0–4) of the different plitidepsin formulations at doses based on MTMD determination (i.e. 0.20 and 0.25 mg/kg for CEW and copolymer formulations, respectively). Tumor size and growth progression, up to day 34, was used to assess the efficacy of therapy. Tumor growth was tracked by regularly measuring the length and width of tumors with a caliper. Tumor volume was calculated using the following equation:

$$V = \frac{\text{length} \times (\text{width})^2}{2}$$

Formulations safety/toxicity was assessed by evaluating body weight variation throughout time.

Data Analysis

A Non-compartmental pharmacokinetic analysis of plitidepsin plasma and organ levels was performed using WinNonlin 5.2 software. Pharmacokinetic parameters were calculated by the log-linear trapezoidal rule (C_{max} values were obtained from observed data). Using the Graphpad Prism 5.0 software, the D'Agostino and Pearson omnibus normality test was used in order to test if data obeyed to a Gaussian distribution. Statistically significant differences between several groups were analyzed by the non-parametric Kruskal-Wallis test, followed by a Dunns post-test. The non-parametric Mann-Whitney test was

used to compare two groups. A p value lower than 0.05 was considered to be statistically significant.

RESULTS

Formulation and Characterization of Loaded Particles

Encapsulation of hydrophobic plitidepsin was explored in both PEG-*b*-PBLG and PTMC-*b*-PGA based particles by co-precipitation using the solvent displacement method. As observed in Table I, the particles produced by this method have a size below 200 nm and a good polydispersity (PDI < 0.2). Moreover, the characteristics of the dispersions were not affected by the presence of plitidepsin up to 30 wt.% FWR for the PEG-*b*-PBLG and 50 wt.% FWR for PTMC-*b*-PGA respectively (see Table I and Fig. 1c and d for PTMC-*b*-PGA and PEG-*b*-PBLG formulations, respectively). Above these values, a macroscopic precipitation was observed. The concentration of plitidepsin in the drug-loaded nanoparticle suspensions was measured by HPLC after solvent extraction. PEG-*b*-PBLG nanoparticles were loaded with maximum 22 wt.% plitidepsin. For PTMC-*b*-PGA, 40 wt.% plitidepsin was measured for a 50 wt.% FWR.

However, in the case of PTMC-*b*-PGA, TEM observations of the highly loaded vesicles (above 20 wt.% FWR) suggested that pure plitidepsin particles were present in a non-negligible amount (Figure S1, Supplementary Material). Indeed, plitidepsin being poorly soluble in water can form particles by nanoprecipitation. This was confirmed by AFM were both plitidepsin particles and polymer vesicles can be distinguished in phase contrast for 40 wt.% FWR (Figure SI-2). Consequently, to both maximize the loading content and avoid the presence of non-encapsulated plitidepsin, FWRs of 30 wt.% and 20 wt.% were chosen for PEG-*b*-PBLG and PTMC-*b*-PGA, respectively.

MTMD Determination

In vivo, the toxicological profiles of the selected nanoparticles were determined by assessing the MTMD in female CD1 mice.

Table III Pharmacokinetic Parameters of Three Different Plitidepsin Formulations in Plasma of Nude Mice Bearing MRI-H-121 Xenografts (average ± SD, n = 4)

Formulation (plitidepsin dose)	C _{max} (ng/mL)	AUC _{0–24 h} (ng·h/mL)	t _{1/2} (h)	CL _p (L/h/kg)	V _{dss} (L/kg)
CEW (0.20 mg/kg)	2.6 ± 0.4	11.6 ± 1.5	8.0 ± 2.1	15.6 ± 1.8	134.2 ± 39.6
PTMC- <i>b</i> -PGA (0.25 mg/kg)	2.4 ± 0.2 (a)	13.0 ± 1.0 (b)	9.9 ± 0.8	16.0 ± 1.1	189.4 ± 21.7 (c)
PEG- <i>b</i> -PBLG (0.25 mg/kg)	8.6 ± 1.3 (a)	24.7 ± 3.2 (b)	8.6 ± 1.3	9.4 ± 1.1	62.5 ± 19.0 (c)

Statistical significance determined between indicated groups: (a) p < 0.025; (b) and (c) p < 0.05

No toxic effects were observed for the unloaded PTMC-*b*-PGA and PEG-*b*-PBLG based nanoparticles, even at the higher dose (i.e. 200 mg/kg), assuring for the non-toxicity of the nanoparticle carriers. As observed in Table II, the MTMD for both drug-loaded particles are marginally higher than the value obtained for the CEW formulation.

To permit an easier comparison between the two nanoparticle formulations the drug dose was set to 0.25 mg/kg for both PTMC-*b*-PGA and PEG-*b*-PBLG in the subsequent studies. Plitidepsin in the reference formulation (i.e. Cremophor® EL/ethanol/water 15/15/70 v/v/v; CEW) was used at maximum MTMD, corresponding to 0.20 mg/kg, following the same administration regime.

Pharmacokinetics

A summary of the pharmacokinetic parameters values derived by a noncompartmental analysis of drug dose in plasma and target organs, after single bolus injection, is presented in Tables III and IV. As observed in Table III, PEG-*b*-PBLG based formulation exhibited superior maximum plasma concentration (C_{max}) and area under the curve (AUC, 0–24 h) while presenting a lower clearance (CL_p) and volume of distribution (V_{dss}), as compared to the other tested formulations. The terminal half-life time ($t_{1/2}$) was equivalent for the three formulations tested (Table III).

Statistically significant differences were observed between PTMC-*b*-PGA and PEG-*b*-PBLG based formulations, the latter presenting higher C_{max} and AUC and lower V_{dss} (Table III).

Tissue analysis revealed comparable tumor C_{max} and AUC for the three different formulations (Table IV).

As means to facilitate comparison between the formulations tested, the C_{max} and AUC₀₋₂₄ values from CEW formulation were normalized to a hypothetical 0.25 mg/kg dose administration. As observed in Table V, the C_{max} in the target tumor tissue was significantly higher for the PTMC-*b*-PGA formulation (in relation with PEG-*b*-PBLG). In the case of the secondary tissues, the CEW formulation C_{max} was significantly higher in kidney, liver and spleen, in relation to correspondent nanoparticle formulation (see Table V). Again and as observed in Table V, the AUC in the target tumor tissue was equivalent for the three different formulations tested. PEG-*b*-PBLG formulation presented significantly higher AUC in plasma (in relation with PTMC-*b*-PGA), while exhibiting significantly lower AUC, as compared to CEW, in off target tissues (i.e. kidney, liver, breast and spleen).

In Vivo Drug Efficacy

Drug efficacy was tested in MRI-H-121 cell tumor bearing athymic nu/nu female mice following five consecutive daily doses (day 0–4) of placebo or plitidepsin formulations (CEW, PTMC-*b*-PGA and PEG-*b*-PBLG at 0.20, 0.25, 0.25 mg/kg, respectively) during 34 days. Tumor volume was measured as means to assess drug formulation antitumor efficacy. As

Table IV Pharmacokinetic Parameters of Three Different Plitidepsin Formulations in Several Tissues of Nude Mice Bearing MRI-H-121 Xenografts (average \pm SD, $n = 4$)

Tissue	CEW (0.20 mg/kg)			PTMC- <i>b</i> -PGA (0.25 mg/kg)			PEG- <i>b</i> -PBLG (0.25 mg/kg)		
	C_{max} (ng/g)	AUC ₀₋₂₄ (ng·h/g)	$t_{1/2}$ (h)	C_{max} (ng/g)	AUC ₀₋₂₄ (ng·h/g)	$t_{1/2}$ (h)	C_{max} (ng/g)	AUC ₀₋₂₄ (ng·h/g)	$t_{1/2}$ (h)
Tumor	58.9 \pm 6.4	956.0 \pm 26.4	28.1 \pm 6.0	77.3 \pm 7.0	1203.7 \pm 263.8	31.7 \pm 9.0	60.0 \pm 4.9	1082.0 \pm 80.5	31.2 \pm 9.5
Kidney	1625.0 \pm 189.8	13921.1 \pm 1845.1	6.6 \pm 2.4	1067.5 \pm 37.7	12204.6 \pm 422.1	7.0 \pm 0.3	1200.8 \pm 325.6	10611.9 \pm 774.5	7.1 \pm 0.5
Liver	2153.5 \pm 281.0	25317.8 \pm 2935.3	8.4 \pm 3.2	1656.7 \pm 210.8	24367.4 \pm 1535.1	8.7 \pm 1.2	1427.0 \pm 75.2	17947.9 \pm 815.9	7.8 \pm 1.8
Breast	91.0 \pm 14.6	1526.6 \pm 200.8	126.2 \pm 47.7	99.9 \pm 22.6	1432.3 \pm 95.1	41 \pm 27.6	80.3 \pm 19.1	1136.0 \pm 109.9	14.7 \pm 8.4
Spleen	1497.5 \pm 669.7	15160.8 \pm 1578.8	16.1 \pm 4.8	1177.5 \pm 170.0	17097.9 \pm 1795.6	15.7 \pm 1.7	1020.8 \pm 84.7	14609.3 \pm 977.4	18.4 \pm 3.6
Intestine	242.5 \pm 34.4	3305.3 \pm 506	10.0 \pm 0.8	360.8 \pm 64.5	5533.0 \pm 314.3	13.5 \pm 3.5	317.8 \pm 71.4	4860.3 \pm 520.5	14.1 \pm 9.1

Table V Maximum Plasma Concentration (C_{max}) and Area under the Curve (AUC) for Three Different Plitidepsin Formulations. CEW Formulation was Normalized to the Maximum used Dose (0.25 mg/kg) to Facilitate Comparison Between Groups (average \pm SD, $n = 4$)

Tissue	CEW (0.25 mg/kg)		PTMC- <i>b</i> -PGA (0.25 mg/kg)		PEG- <i>b</i> -PBLG (0.25 mg/kg)	
	C_{max} (ng/g)	AUC ₀₋₂₄ (ng · h/g)	C_{max} (ng/g)	AUC ₀₋₂₄ (ng · h/g)	C_{max} (ng/g)	AUC ₀₋₂₄ (ng · h/g)
Plasma	3.2 \pm 0.5	14.5 \pm 1.9	2.4 \pm 0.2(a)	13.0 \pm 1.0(b)	8.6 \pm 1.3(a)	24.7 \pm 3.2(b)
Tumor	73.6 \pm 8.0	1195.0 \pm 33.1	77.3 \pm 7.0(c)	1203.7 \pm 263.8	60.0 \pm 4.9(c)	1082.0 \pm 80.5
Kidney	2031 \pm 237.3(d)	17401.4 \pm 2306.4(e)	1067.5 \pm 37.7(d)	12204.6 \pm 422.1	1200.8 \pm 325.6	10611.9 \pm 774.5(e)
Liver	2692.0 \pm 351.2(f)	31647.2 \pm 3669.2(g)	1656.7 \pm 210.8	24367.4 \pm 1535.1	1427.0 \pm 75.2(f)	17947.9 \pm 815.9(g)
Breast	113.8 \pm 18.3	1908.3 \pm 251.0(h)	99.9 \pm 22.6	1432.3 \pm 95.1	80.3 \pm 19.1	1136.0 \pm 109.9(h)
Spleen	1872 \pm 837.1(i)	18950.9 \pm 1973.5(j)	1177.5 \pm 170.0	17097.9 \pm 1795.6	1020.8 \pm 84.7(i)	14609.3 \pm 977.4(j)
Intestine	303.2 \pm 43.0	4131.6 \pm 632.5(k)	360.8 \pm 64.5	5533.0 \pm 314.3(k)	317.8 \pm 71.4	4860.3 \pm 520.5

Statistical significance differences determined between indicated groups

(a), (e), (g) $p < 0.025$; (b), (c), (d), (f), (h), (i), (j), (k) $p < 0.05$

observed in Fig. 2, a significant tumor size difference was observed between the placebo and plitidepsin formulations for time points between 2 and 27 days. Animal body weight surveillance was performed to detect eventual treatment acute toxicity. No significant differences were observed in terms of animal weigh progression between the groups, during the time course of the study (see Figure S3 in Supplementary Material). The survival rate in all test groups was 100%.

DISCUSSION

Here and by means of plitidepsin encapsulation in nanosized platforms, whether in a vesicular or micellar structure (PTMC-*b*-PGA or PEG-*b*-PBLG, respectively), we aimed to assess if significant improvements in terms of drug circulation time and

drug efficacy could be achieved, using a ectopic renal cancer model. Nanoparticle preparation was performed using the nanoprecipitation method (solvent assisted dispersion). This simple method allows the preparation of drug-loaded nanoparticles in one step with a good control over size and size dispersity as well as reasonable reproducibility and scalability. The obtained nanoparticles presented sizes below 200 nm, making them appropriate for parenteral administration. Additionally, the preparation method allowed high plitidepsin loading contents (15 and 22% for PTMC-*b*-PGA and PEG-*b*-PBLG, respectively). Interestingly, PTMC-*b*-PGA and PEG-*b*-PBLG presented a rather different behavior concerning plitidepsin loading. In the case of PEG-*b*-PBLG, stable micelle-like particles were formed up to 30 wt.% FWRs. Above this value, micro-sized objects that tended to rapidly flocculate were produced, whereas for PTMC-*b*-PGA, FWRs above 20 wt.% did not lead to an increase of the vesicles size. However, TEM and AFM observations revealed that small particles of non-encapsulated plitidepsin were formed for FWRs of 40 wt.%, establishing the 20 wt.% for the subsequent studies.

As shown by the biodistribution studies, the PEG-*b*-PBLG formulation demonstrated superior C_{max} and AUC. Additionally, the same formulation presented lower clearance (CL_p) and volume of distribution at steady state (V_{dss}) indicating lower extravasation to off target tissues, particularly the reticular endothelial system and the renal pathway. Indeed, the AUC in liver, kidney, spleen and breast was significantly reduced, compared to CEW formulation. The inclusion of PEG moieties to nanoparticle surface was already reported to increase encapsulated drug half life together with a concomitant uptake reduction from the mononuclear phagocytic system (29). In a recent work, Alonso and colleagues have shown that the nanoencapsulation of plitidepsin using pegylated PGA nanocapsules presented a higher half-life time, mean residence time and AUC, as compared with PGA alone (30).

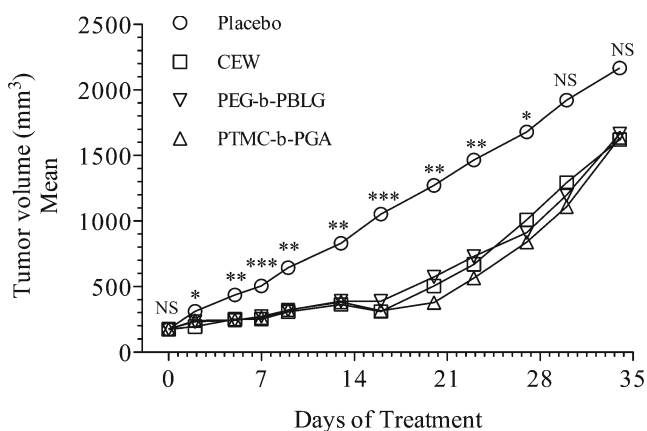


Fig. 2 Tumor volume progression of MRI-H-121 cell tumor bearing athymic nu/nu female mice, following five consecutive daily doses (day 0–4) of placebo or plitidepsin formulations: CEW (0.20 mg/kg), PTMC-*b*-PGA (0.25 mg/kg) or PEG-*b*-PBLG (0.25 mg/kg) during 34 days (mean; $n = 8$; *, ** and *** denotes $p < 0.05$, $p < 0.01$ and $p < 0.001$, respectively; NS denotes non significant).

Pegylation has for long been applied to liposomal (31) and nanoparticle (32) systems in order to improve drug delivery systems performance upon administration *in vivo*.

Motivated by the biodistribution profiles we moved to test the efficacy of such formulations using an ectopic renal cancer model. The encapsulation of plitidepsin in the form of micelles or vesicles allowed increasing the MTMD from 0.2 (corresponding to CEW formulation) to 0.25 mg/Kg, for PEG-*b*-PBLG and PTMC-*b*-PGA.

The three tested formulations demonstrated similar tumor regression efficiency. In spite of the unique biodistribution profile, the PEG-*b*-PBLG formulation was not able to improve the overall treatment efficiency. Indeed, no significant improvements could be achieved in terms of tumor regression, in relation with current CEW formulations. However, due to the unique biodistribution profile of PEG-*b*-PBLG plitidepsin loaded formulation one can envisage reduced unwanted side effects of plitidepsin *in vivo*. Additionally, and according to the body weight evaluation no relevant acute toxicity was elicited by the nanoparticle based systems, reinforced by the survival rate of 100%.

CONCLUSIONS

Pharmacokinetic and biodistribution parameters were modified following the administration of copolymer-based formulations, i.e., PEG-*b*-PBLG formulation. However changes on pharmacokinetics and biodistribution profiles did not translate into different antitumor activity *in vivo*. Nonetheless, this approach demonstrated the potential of copolymer-based nanoparticles as novel plitidepsin delivery systems. Due to the hydrophobic character of plitidepsin it is required the use of adjuvants in order to permit *iv.* administration. The nano encapsulation of plitidepsin allowed the maintenance of the therapeutic efficacy, while reducing off target tissue distribution. Here we demonstrated the potential of amphiphilic block copolymers for the encapsulation of a highly hydrophobic anticancer drug, using a simple process (i.e. nanoprecipitation). Additionally, and due to the non-toxicity of the vehicles (empty nanoparticles showed a MTMD higher than 200 mg/Kg) the developed systems present clinical relevant alternatives to the current CEW formulation, as they display improved biodistribution profiles what may diminish potential unwanted side effects.

ACKNOWLEDGMENTS AND DISCLOSURES

This work was supported by funding from the European Commission under the seventh framework within the frame of the NanoTher project (Integration of novel NANOparticle based technology for THERapeutics and diagnosis of different types of cancer CP-IP 213631-2).

REFERENCES

- Davis ME, Chen ZG, Shin DM. Nanoparticle therapeutics: an emerging treatment modality for cancer. *Nat Rev Drug Discov.* 2008;7:771–82.
- Alexis F, Pridgen EM, Langer R, Farokhzad OC. Nanoparticle technologies for cancer therapy. *Handb Exp Pharmacol.* 2010;197: 55–86.
- De Oliveira H, Thevenot J, Lecommandoux S. Smart polymersomes for therapy and diagnosis: fast progress toward multifunctional biomimetic nanomedicines. *Wiley Interdiscip Rev Nanomed Nanobiotechnol.* 2012;4:525–46.
- Rinehart K, Lithgow-Berelloni AM. Novel antiviral and cytotoxic agent. PCT Int. Pat. Appl. WO 91.04985, Apr. 18, 1991K; GB Appl. 89/22,026, Sept, 515 29, 1989; International patent number: 115:248086q.
- Mitsiades CS, Ocio EM, Pandiella A, Maiso P, Gajate C, Garayoa M, et al. Aplidin, a marine organism-derived compound with potent antimyeloma activity *in vitro* and *in vivo*. *Cancer Res.* 2008;68:5216–25.
- Caers J, Menu E, De Raeye H, Lepage D, Van Valckenborgh E, Van Camp B, et al. Antitumour and antiangiogenic effects of Aplidin in the 5TMM syngeneic models of multiple myeloma. *Br J Cancer.* 2008;98:1966–74.
- Straight AM, Oakley K, Moores R, Bauer AJ, Patel A, Tuttle RM, et al. Aplidin reduces growth of anaplastic thyroid cancer xenografts and the expression of several angiogenic genes. *Cancer Chemother Pharmacol.* 2006;57:7–14.
- Gonzalez-Santiago L, Suarez Y, Zarich N, Munoz-Alonso MJ, Cuadrado A, Martinez T, et al. Aplidin induces JNK-dependent apoptosis in human breast cancer cells via alteration of glutathione homeostasis, Rac1 GTPase activation, and MKP-1 phosphorylation. *Cell Death Differ.* 2006;13:1968–81.
- Garcia-Fernandez LF, Losada A, Alcaide V, Alvarez AM, Cuadrado A, Gonzalez L, et al. Aplidin induces the mitochondrial apoptotic pathway via oxidative stress-mediated JNK and p38 activation and protein kinase C delta. *Oncogene.* 2002;21:7533–44.
- Cuadrado A, Gonzalez L, Suarez Y, Martinez T, Munoz A. JNK activation is critical for Aplidin-induced apoptosis. *Oncogene.* 2004;23:4673–80.
- Faivre S, Chieze S, Delbaldo C, Ady-Vago N, Guzman C, Lopez-Lazaro L, et al. Phase I and pharmacokinetic study of aplidine, a new marine cyclodepsipeptide in patients with advanced malignancies. *J Clin Oncol.* 2005;23:7871–80.
- Maroun JA, Belanger K, Seymour L, Matthews S, Roach J, Dionne J, et al. Phase I study of Aplidine in a dailyx5 one-hour infusion every 3 weeks in patients with solid tumors refractory to standard therapy. A National Cancer Institute of Canada Clinical Trials Group study: NCIC CTG IND 115. *Ann Oncol.* 2006;17:1371–8.
- Izquierdo MA, Bowman A, Garcia M, Jodrell D, Martinez M, Pardo B, et al. Phase I clinical and pharmacokinetic study of plitidepsin as a 1-hour weekly intravenous infusion in patients with advanced solid tumors. *Clin Cancer Res.* 2008;14:3105–12.
- Schoffski P, Guillem V, Garcia M, Rivera F, Tabernero J, Cullell M, et al. Phase II randomized study of Plitidepsin (Aplidin), alone or in association with L-carnitine, in patients with unresectable advanced renal cell carcinoma. *Mar Drugs.* 2009;7:57–70.
- Eisen T, Thatcher N, Leyvraz S, Miller Jr WH, Couture F, Lorigan P, et al. Phase II study of weekly plitidepsin as second-line therapy for small cell lung cancer. *Lung Cancer.* 2009;64:60–5.
- Eisen T, Thomas J, Miller Jr WH, Gore M, Wolter P, Kavan P, et al. Phase II study of biweekly plitidepsin as second-line therapy in patients with advanced malignant melanoma. *Melanoma Res.* 2009;19:185–92.
- Dumez H, Gallardo E, Culine S, Galceran JC, Schoffski P, Droz JP, et al. Phase II study of biweekly plitidepsin as second-line therapy for

- advanced or metastatic transitional cell carcinoma of the urothelium. *Mar Drugs*. 2009;7:451–63.
18. Baudin E, Droz JP, Paz-Ares L, van Oosterom AT, Cullell-Young M, Schlumberger M. Phase II study of plitidepsin 3-hour infusion every 2 weeks in patients with unresectable advanced medullary thyroid carcinoma. *Am J Clin Oncol*. 2010;33:83–8.
 19. Peschel C, Hartmann JT, Schmittl A, Bokemeyer C, Schneller F, Keilholz U, *et al.* Phase II study of plitidepsin in pretreated patients with locally advanced or metastatic non-small cell lung cancer. *Lung Cancer*. 2008;60:374–80.
 20. Mateos MV, Cibeira MT, Richardson PG, Prosper F, Oriol A, de la Rubia J, *et al.* Phase II clinical and pharmacokinetic study of plitidepsin 3-hour infusion every two weeks alone or with dexamethasone in relapsed and refractory multiple myeloma. *Clin Cancer Res*. 2010;16:3260–9.
 21. Ribrag V, Caballero D, Ferme C, Zucca E, Arranz R, Briones J, *et al.* Multicenter phase II study of plitidepsin in patients with relapsed/refractory non-Hodgkin's lymphoma. *Haematologica*. 2013;98(3):357–63.
 22. Weiss RB, Donehower RC, Wiernik PH, Ohnuma T, Gralla RJ, Trump DL, *et al.* Hypersensitivity reactions from taxol. *J Clin Oncol*. 1990;8:1263–8.
 23. Gelderblom H, Verweij J, Nooter K, Sparreboom A. Cremophor EL: the drawbacks and advantages of vehicle selection for drug formulation. *Eur J Cancer*. 2001;37:1590–8.
 24. Bristol-Myers Squibb Co. Princeton. Taxol® (paclitaxel) Injection. March 2003. Available from: <http://www.accessdata.fda>.
 25. Bazile D, Prud'homme C, Bassoullet MT, Marlard M, Spenlehauer G, Veillard M. Stealth Me.PEG-PLA nanoparticles avoid uptake by the mononuclear phagocytes system. *J Pharm Sci*. 1995;84:493–8.
 26. Nuijen B, Bouma M, Henrar RE, Manada C, Bult A, Beijnen JH. Compatibility and stability of aplidine, a novel marine-derived depsipeptide antitumor agent, in infusion devices, and its hemolytic and precipitation potential upon i.v. administration. *Anticancer Drugs*. 1999;10:879–87.
 27. Barbosa MEM, Montembault V, Cammas-Marion S, Ponchel G, Fontaine L. Synthesis and characterization of novel poly(γ -benzyl-L-glutamate) derivatives tailored for the preparation of nanoparticles of pharmaceutical interest. *Polym Int*. 2007;56:317–24.
 28. Sanson C, Schatz C, Le Meins J-FO, Brûlet A, Soum A, Lecommandoux SB. Biocompatible and Biodegradable Poly(trimethylene carbonate)-*b*-Poly(L-glutamic acid) Polymersomes: Size Control and Stability. *Langmuir*. 2009;26:2751–60.
 29. 3rd Owens DE, Peppas NA. Opsonization, biodistribution, and pharmacokinetics of polymeric nanoparticles. *Int J Pharm*. 2006;307:93–102.
 30. Gonzalo T, Lollo G, Garcia-Fuentes M, Torres D, Correa J, Riguera R, *et al.* A new potential nano-oncological therapy based on polyamino acid nanocapsules. *J Control Release*. 2013;169:10–6.
 31. Papahadjopoulos D, Allen TM, Gabizon A, Mayhew E, Matthay K, Huang SK, *et al.* Sterically stabilized liposomes: improvements in pharmacokinetics and antitumor therapeutic efficacy. *Proc Natl Acad Sci U S A*. 1991;88:11460–4.
 32. Gref R, Minamitake Y, Peracchia MT, Trubetskoy V, Torchilin V, Langer R. Biodegradable long-circulating polymeric nanospheres. *Science*. 1994;263:1600–3.